Nematode m^7GpppG and $m_3^{2,2,7}GpppG$ decapping: Activities in *Ascaris* embryos and characterization of *C. elegans* scavenger DcpS

LEAH S. COHEN,[1] CLAUDETTE MIKHLI,[1] CASSANDRA FRIEDMAN,[1] MARZENA JANKOWSKA–ANYSZKA,[2] JANUSZ STEPINSKI,[3] EDWARD DARZYNKIEWICZ,[3] and RICHARD E. DAVIS[1]

[1]Department of Biology, City University of New York (CUNY) Graduate Center, Staten Island, New York 10314, USA
[2]Department of Chemistry and [3]Department of Biophysics, University of Warsaw, 02-089 Warsaw, Poland

ABSTRACT

A spliced leader contributes the mature 5′ ends of many mRNAs in *trans*-splicing organisms. *Trans*-spliced metazoan mRNAs acquire an $m_3^{2,2,7}GpppN$ cap from the added spliced leader exon. The presence of these caps, along with the typical m^7GpppN cap on non-*trans*-spliced mRNAs, requires that cellular mRNA cap-binding proteins and mRNA metabolism deal with different cap structures. We have developed and used an in vitro system to examine mRNA degradation and decapping activities in nematode embryo extracts. The predominant pathway of mRNA decay is a 3′ to 5′ pathway with exoribonuclease degradation of the RNA followed by hydrolysis of resulting mRNA cap by a scavenger (DcpS-like) decapping activity. Direct decapping of mRNA by a Dcp1/Dcp2-like activity does occur, but is ~15-fold less active than the 3′ to 5′ pathway. The DcpS-like activity in nematode embryo extracts hydrolyzes both m^7GpppG and $m_3^{2,2,7}GpppG$ dinucleoside triphosphates. The Dcp1/Dcp2-like activity in extracts also hydrolyzes these two cap structures at the 5′ ends of RNAs. Interestingly, recombinant nematode DcpS differs from its human ortholog in its substrate length requirement and in its capacity to hydrolyze $m_3^{2,2,7}GpppG$.

Keywords: decapping; *in vitro* RNA decay; scavenger; DcpS; m^7GpppG, $m_3^{2,2,7}GpppG$; trimethylguanosine (TMG) cap; Dcp1/Dcp2; nematode; *Ascaris*; *C. elegans*

INTRODUCTION

Spliced leader (SL) RNA *trans*-splicing contributes a 5′ terminal exon to pre-mRNAs to form the mature 5′ end of the mRNA. SL *trans*-splicing is present in a diverse spectrum of eukaryotes including sarcomastigophoran protozoa (euglenoids and trypanosomes and their relatives), Cnidaria (*Hydra vulgaris*), flatworms (free-living and parasitic: polyclads, flukes, and tapeworms), nematodes (e.g., *Caenorhabditis elegans* and *Ascaris*), and chordates (tunicate, *Ciona intestinalis*; Nilsen 2001). Addition of the 5′ terminal exon from *trans*-splicing SL RNAs generates cellular mRNAs with a short, conserved sequence in the mRNA 5′ untranslated region (UTR) and a distinct hypermethylated cap (in metazoa) derived from the donated spliced leader, an $N^{2,2,7}$-trimethyl-GpppN cap ($m_3^{2,2,7}GpppN$ or TMG cap). Non-*trans*-spliced mRNAs have an N^7-methyl-GpppN RNA cap (m^7GpppN) with diverse 5′ UTR sequences. Therefore, two populations of mRNAs coexist in metazoan cells that exhibit spliced leader addition: *trans*-spliced and non-*trans*-spliced mRNAs.

Both mRNA cap and 5′ UTR sequence and structure are known to play important roles in translation, and cap structure is also an important determinant in transcript stability. The mRNA cap is recognized and bound directly or indirectly by a number of different cap-binding proteins. Cap-binding or -interacting proteins include the translation initiation factor eIF4E (Gingras et al. 1999; Von Der Haar et al. 2004), nuclear cap-binding complex (consisting of cap-binding proteins CBP 20 and 80; Izaurralde et al. 1994, 1995), and decapping proteins (Dcp1, Dcp2, and DcpS; for review, see Decker and Parker 2002). Proteins that interact with the metazoan hypermethylated cap ($m_3^{2,2,7}GpppN$)

Reprint requests to (current address): Richard E. Davis, Departments of Biochemistry and Molecular Genetics and Pediatrics, UCHSC, Mail Stop 8101, P.O. Box 6511, 12801 East 17th Avenue, Aurora, CO 80045, USA; e-mail: Richard.Davis@uchsc.edu; fax: (303) 724-3215.

Article and publication are at http://www.rnajournal.org/cgi/doi/10.1261/rna.7690504.

and/or spliced leader sequence of a *trans*-spliced mRNA are likely to play an important role in mRNA metabolism, and may mediate the use and/or cellular discrimination of *trans*-spliced versus non-*trans*-spliced mRNAs.

Decapping proteins are involved in cleaving the unusual 5′-ppp-5′ phosphodiester linkage in the RNA cap (G-$^{5'}$ppp$^{5'}$-N). The presence of the RNA cap triphosphate bridge increases mRNA stability presumably as it prevents 5′ to 3′ exoribonuclease degradation of the mRNA. mRNA decay pathways have been extensively characterized in yeast and more recently in higher eukaryotes. A major mechanism of mRNA decay in yeast proceeds from 5′ to 3′ following removal of the cap. Decay is initiated by deadenylation of the mRNA (Tucker and Parker 2000; Parker and Song 2004). This typically leads to decapping of the intact RNA by a protein complex known as Dcp1/Dcp2 (Beelman et al. 1996; Dunckley and Parker 1999; Parker and Song 2004). Removal of the cap exposes the 5′ end of the RNA to exoribonucleolytic decay by Xrn1. A second general pathway, often called the 3′ to 5′ pathway, involves deadenylation of the mRNA followed by 3′ to 5′ exoribonuclease degradation of the mRNA body by the exosome (Tucker and Parker 2000; Parker and Song 2004). Processive 3′ to 5′ degradation of the mRNA body finally leads to the production of a 5′ cap dinucleoside triphosphate (m^7GpppN or short m^7GpppN capped oligonucleotide). The m^7GpppN or oligonucleotide cap is subsequently hydrolyzed by what has been named a "scavenger" decapping activity (DcpS; Nuss et al. 1975; Wang and Kiledjian 2001; Liu et al. 2002). The 3′ to 5′ pathway is typically considered a less active pathway for mRNA turnover in yeast. However, a recent genome-wide analysis of mRNA decay using expression profiling and various mutant yeast strains suggests the possibility that the 3′ to 5′ decay may be more important than previously realized (He et al. 2003). Yeast cells blocked in both the 5′ to 3′ and 3′ to 5′ pathways are not viable, illustrating the importance of mRNA turnover in gene expression (Anderson and Parker 1998).

The predominant general pathway of mRNA decay in higher eukaryotes is currently unclear. Experiments using mammalian cells, and particularly in vitro studies, suggest that an important mechanism is through the 3′ to 5′ decay pathway (Chen et al. 2001; Wang and Kiledjian 2001; Mukherjee et al. 2002) leading to cap dinucleoside triphosphate, m^7GpppN, which is cleaved by the scavenger activity (DcpS; Wang and Kiledjian 2001). Both types of decapping activity, DcpS and Dcp1/Dcp2, have been described in mammalian cells (Gao et al. 2001; Wang and Kiledjian 2001; Wang et al. 2002; Lejeune et al. 2003). A recent RNAi study demonstrated that the *C. elegans* 5′ to 3′ exoribonuclease is required in the latter stages of embryogenesis when epithelial cell movements are required for ventral closure (Newbury and Woollard 2004). Overall, however, the nature and contribution of different mRNA decay pathways and decapping enzymes to mRNA turnover and their importance in development or viability in multicellular organisms have not been characterized.

SL1 *trans*-splicing is responsible for the maturation of ~50 to 90% of mRNAs in the nematodes *C. elegans* and *Ascaris*, respectively (Zorio et al. 1994; Maroney et al. 1995). The function(s) of SL1 *trans*-splicing in nematode gene expression remains unknown. Among the possible post-transcriptional functions that have been postulated for addition of the TMG-capped-SL sequence to mRNAs are roles in mRNA translation, stability, processing, localization, and/or transport. SL1 *trans*-splicing is required for early *C. elegans* development (Ferguson et al. 1996), and the SL1 sequence with its TMG cap have been shown to functionally collaborate to enhance translational efficiency of a *trans*-spliced mRNA in an in vitro system (Maroney et al. 1995). However, our in vitro and in vivo translation studies in *Ascaris* embryos indicate that the TMG-capped-SL sequence does not confer a measurable translational advantage on recipient mRNAs (L.S. Cohen, M. Mikhli, C. Friedman, M. Jankowska-Anyszka, J. Stepinski, E. Darzynkiewicz, and R.E. Davis, unpubl.; S. Lall, C. Friedman, M. Jankowska-Anyszka, J. Stepinski, E. Darzynkiewicz, and R.E. Davis, in prep.). A second SL sequence (SL2) with a hypermethylated cap and sequence divergent from SL1 (~50% sequence similarity) is also present in *C. elegans* (Huang and Hirsh 1989). SL2 is added to internal splice acceptor sites between mRNAs in polycistronic primary trancripts contributing to the maturation of these operon RNAs into monocistronic mRNAs (Spieth et al. 1993; Blumenthal and Gleason 2003). Although SL1 *trans*-splicing is capable of resolving polycistronic transcripts under some conditions, it is unclear whether this is a primary function of SL1 *trans*-splicing and the overall function of SL1 remains unclear (Williams et al. 1999; Liu et al. 2001).

Several decapping enzymes that hydrolyze the m^7GpppN cap on mRNAs or free cap dinucleoside triphosphates have recently been characterized in yeast and mammalian cells (Beelman et al. 1996; LaGrandeur and Parker 1998; Dunckley and Parker 1999; Wang and Kiledjian 2001; Liu et al. 2002; Lykke-Andersen 2002; Salehi et al. 2002; van Dijk et al. 2002, 2003; Wang et al. 2002; Piccirillo et al. 2003). mRNA decay, deadenylation, and decapping activities have also recently been described in trypanosomes (Milone et al. 2002, 2004). However, activities in other species have not been well characterized, and neither mRNA decay pathways nor decapping activities have been examined directly in *trans*-splicing metazoa. In *trans*-splicing metazoa, the two distinctly capped mRNA populations, and particularly the presence of a distinct cap and the SL sequence on some mRNAs may have a profound influence on mRNA translation and stability. Analysis of the decay pathways and associated proteins may provide insight into the function of *trans*-splicing, and could lead to potential targets for rational drug design against a number of divergent parasitic worms. In this paper, we describe mRNA transcript decay

that yields mRNA caps as well as the m^7GpppG and $m_3^{2,2,7}$GpppG decapping activities present in nematodes using *Ascaris* embryo extracts. We have also produced and characterized a recombinant *C. elegans* dinucleoside triphosphate scavenger type decapping protein (DcpS) that can hydrolyze m^7GpppG and $m_3^{2,2,7}$GpppG.

RESULTS

Decay and decapping activity in *Ascaris* embryo whole cell extracts

Two distinct mRNA cap-cleaving activities have been described in eukaryotes. One activity, Dcp1/Dcp2, decaps m^7GpppN-mRNA substrates producing m^7Gpp + pN-RNA products (Beelman et al. 1996; Lykke-Andersen 2002; van Dijk et al. 2002; Wang et al. 2002; Steiger et al. 2003). A second activity described as a scavenger activity, DcpS, hydrolyzes N^7–methyl-guanosine-dinucleoside triphosphate (m^7GpppN) or a short oligonucleotide cap (m^7GpppN$_n$) producing m^7Gp and ppN products (Nuss et al. 1975; Nuss and Furuichi 1977; Wang and Kiledjian 2001; Liu et al. 2002). These two cap cleaving activities can be distinguished by their reaction products, m^7Gp for the scavenger/dinucleoside triphosphate activity (DcpS) and m^7Gpp for the Dcp1/Dcp2 RNA decapping activity.

We prepared *Ascaris* embryo extracts competent for cap-dependent translation that demonstrate cap and poly(A)-tail translation synergism (S. Lall, C. Friedman, M. Jankowska-Anyszka, J. Stepinski, E. Darzynkiewicz, and R.E. Davis, in prep.). These extracts were considered to be physiologically relevant for analysis of decapping activities and mRNA turnover. Cap-labeled m^7Gp*ppG-RNA (where the * follows the ^{32}P-labeled phosphate) was incubated in 32–64 cell *Ascaris* embryo extracts for 30–60 min and the decay and decapping reaction products characterized by thin layer chromatography and PAGE. Analysis of the reaction products derived from incubation of a 250 nucleotide cap-labeled m^7Gp*ppG-Ren$_{250}$-RNA (derived from pRLnull; see Supplementary Fig. 1) indicated that the predominant RNA decapping product observed was m^7Gp* (Fig. 1A, lane 2). The decay and decapping reactions are linear for at least 30 min, and dependent on extract con-

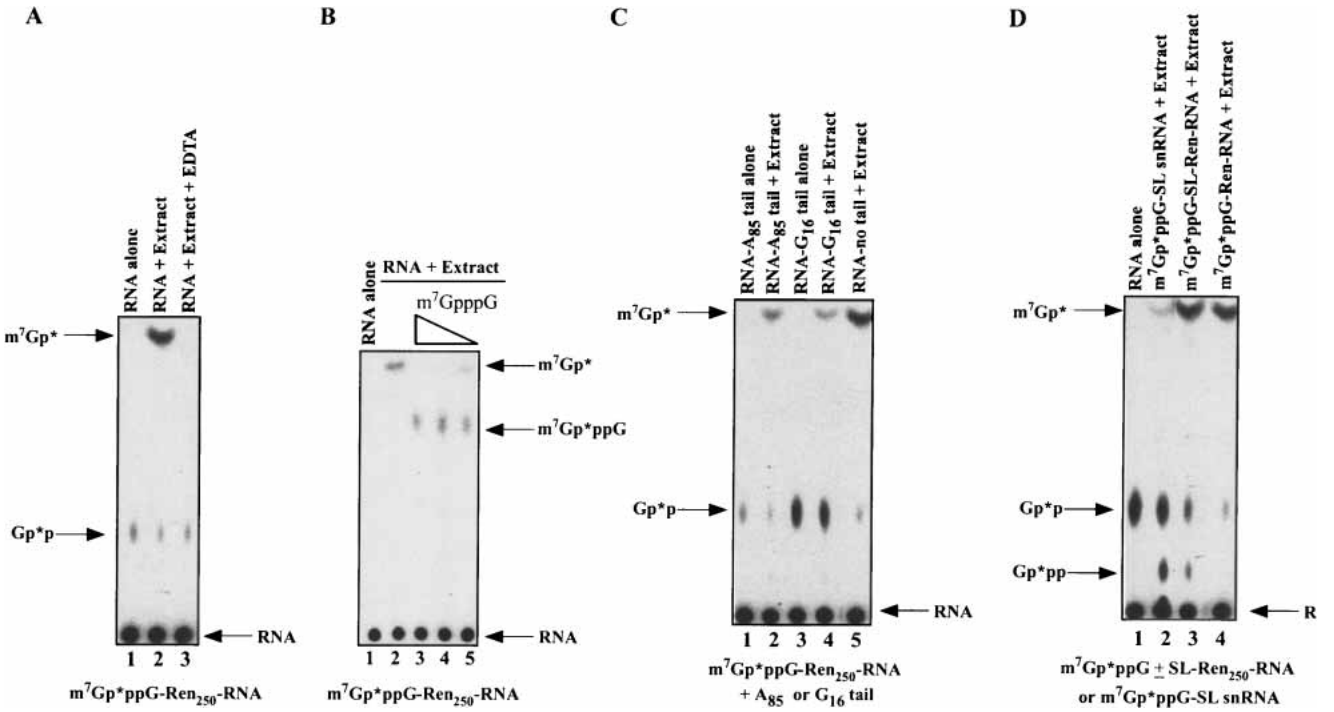

FIGURE 1. RNA decay and decapping activity in *Ascaris* embryo extracts illustrates contribution of 3′ to 5′ exoribonuclease and scavenger activities. (*A*) m^7Gp*ppG ^{32}P-cap-labeled RNA undergoes decay and decapping in *Ascaris* extracts producing m^7Gp*. A 250 nucleotide cap-labeled RNA substrate (the * follows the ^{32}P-labeled phosphate) derived from the 5′ end of pRLnull was incubated in *Ascaris* embryo extract for 50 min at 30°C, aliquots of the reactions were then applied to PEI-cellulose thin layer chromatography (TLC) plates, the plates developed in 0.45 M ammonium sulfate, and labeled substrate and products detected by autoradiography. Comigration of appropriate markers followed by UV shadowing, enzymatic conversion assays, and inhibition studies were used to identify and confirm reaction products. Note that the Gp*p spot is derived from the cap-labeling reaction and is not present in gel-purified RNA substrates that were used in other experiments with similar results. (*B*) Inhibition of scavenger activity during RNA decay leads to accumulation of m^7GpppG in *Ascaris* extracts. Reactions were carried out with or without cap analogs. Concentrations of competitive cap inhibitors are 200, 50, and 20 μM. (*C*) Addition of a 3′ poly(A)-tail or G_{16} to the RNA substrate leads to reduction in m^7Gp* product. (*D*) Inherent SL snRNA structure and SL RNP formation in *Ascaris* extracts leads to a reduction in decay and scavenger product. Note that the SL snRNA undergoes reduced decay and cap hydrolysis (cf. lane *2* and lanes *3,4*), while an mRNA with only the m^7Gp*ppG-capped 22 nucleotide SL sequence added to its 5′ end is degraded and hydrolyzed normally (cf. lanes *3* and *4*). RNA alone = m^7Gp*ppG-SL snRNA. Reactions in (*B*)–(*D*) were carried out and analyzed as described in (*A*).

centration (data not shown). Similar results were obtained using an ~1 kb RNA with a complete open reading frame and poly(A)-tail and an actin mRNA (data not shown).

Several lines of evidence suggest that the m^7Gp^* product observed in the whole cell extract decay reactions results from (1) 3′ to 5′ exoribonucleolytic decay of the RNA producing a short m^7Gp^*ppG substrate that is (2) rapidly cleaved by a dinucleoside triphosphate hydrolase ("scavenger" or DcpS-like) activity. The exosome and 3′ to 5′ exoribonucleolytic RNA decay in other systems are known to require Mg^{++} and are inhibited by EDTA. Notably, m^7Gp^* derived from RNA substrates in the *Ascaris* embryo extracts is greatly reduced in the presence of EDTA (Fig. 1A, cf. lanes 2 and 3), suggesting that the RNA decay or scavenger activity is inhibited. Under our RNA decay assay conditions, the m^7Gp^*ppG product derived from 3′ to 5′ exoribonucleolytic decay of the RNA—and the substrate of the scavenger activity—does not accumulate in the reactions. m^7Gp^*ppG substrate (or short cap oligonucleotides) accumulates in RNA decay reactions when DcpS activity is specifically inhibited by m^7GpppG cap or m^7Gpp nucleotides or in extract fractions with reduced scavenger dinucleoside triphosphate hydrolase activity (Fig. 1B, cf. lane 2 and lanes 3–5; e.g., S130 pellet; see below). Because our analysis of recombinant nematode DcpS scavenger activity indicates that it does not require Mg^{++} or Mn^{++} (data not shown), these data support the existence of an EDTA inhibited 3′ to 5′ exoribonucleolytic pathway that generates substrate for the scavenger-like enzyme.

RNA elements and/or RNA binding proteins that decrease 3′ to 5′ exoribonucleolytic decay of an RNA should lead to less m^7Gp^*ppG product generated by the exosome, reducing substrate available for the scavenger decapping activity, and a consequent reduction in m^7Gp^* product. Addition of either an 85 nucleotide poly(A)-tail or G_{16} to the 3′ end of the RNA, sequences known to reduce 3′ to 5′ exonucleolytic decay of RNA substrates, did lead to a decrease in m^7Gp^* product (Fig. 1C, cf. lane 5 and lanes 2,4). The most striking example of decreased m^7Gp^* product as a result of decreased 3′ to 5′ exoribonucleolytic decay is observed when the spliced leader RNA (SL snRNA) is the substrate. This small 110 nucleotide RNA is predicted to form a three-stem-loop structure, and is known to assemble into a complex SL RNP in *Ascaris* embryo extracts (Maroney et al. 1990a; Denker et al. 1996, 2002). We predict this SL RNP would be relatively resistant to 3′ to 5′ exoribonucleolytic decay, leading to minimal m^7Gp^*ppG substrate formation. As predicted, low levels of m^7Gp^* were generated in the extracts from the SL snRNA substrate (Fig. 1D, cf. lanes 2 and 4). Addition of the spliced leader sequence alone to the 5′ end of a truncated mRNA is not predicted to lead to the formation of a complex structure and RNP, and does not similarly reduce m^7Gp^* formation (Fig. 1D, cf. lane 3 and lanes 2,4). We interpret the sum of these observations (EDTA inhibition of the 3′ to 5′ decay, m^7GpppG accumulation following inhibition of scavenger activity, and 3′ poly(A) or (G) and SL snRNP structure leading to reduction in m^7Gp^* formation) to indicate that the rate-limiting step in the complete decay of the RNA in these reactions is the 3′ to 5′ exoribonucleolytic decay of the RNA. In support of this interpretation, incubation of a labeled RNA containing a 3′ subterminal G_{16} or G_{30} tract in the extract leads to the predicted 3′–5′ decay intermediate stalled at the G-tracts as shown in other systems (data not shown; Anderson and Parker 1998; Milone et al. 2002)

The combined activity of 3′ to 5′ exoribonucleolytic decay and scavenger cleavage of the resulting cap dinucleoside triphosphate product were observed on a number of different RNA substrates. In addition, similar decay, RNA decapping, and dinucleoside triphosphate hydrolase activities were also observed in *C. elegans* whole cell embryo extracts (Supplementary Fig. 2F; data not shown).

Decay and decapping of $m_3^{2,2,7}GpppG$-capped RNAs

Both $m_3^{2,2,7}GpppG$- and m^7GpppN-capped mRNAs are substrates for RNA decay in nematodes. To determine whether the scavenger activity in the nematode extracts could cleave an $m_3^{2,2,7}Gp^*ppG$ cap substrate, a cap-labeled trimethylguanosine ($m_3^{2,2,7}Gp^*ppG$) RNA was prepared by hypermethylation of an m^7Gp^*ppG cap-labeled SL snRNA in *Ascaris* embryo extracts as previously described (Maroney et al. 1990a). SL snRNA hypermethylation is not complete in these reactions, leading to a mixed substrate containing $m^7Gp^*ppG_m$ and $m_3^{2,2,7}Gp^*ppG_m$ capped SL snRNAs as deduced from nuclease P1 and T1 digestion and TLC and PAGE analysis of the products (Fig. 2A, lane 3; Supplementary Fig. 2B,C; data not shown). Incubation of the mono- and tri-methyl-capped-SL snRNAs in whole cell *Ascaris* embryo extracts resulted in the accumulation of both m^7Gp^* and $m_3^{2,2,7}Gp^*$ products (Fig. 2A, lane 5; Fig. 2B, lane 1). 3′ to 5′ exoribonucleolytic decay of these RNAs should lead to the formation of both $m_3^{2,2,7}GpppG$ and m^7GpppG dinucleoside triphosphates. When nematode scavenger activity is inhibited in the extract with 100 μM m^7GDP, both $m_3^{2,2,7}GpppG$ and m^7GpppG dinucleoside triphosphates accumulate from $m_3^{2,2,7}GpppG$ and m^7GpppG capped RNAs (Fig. 2B, lane 2). Overall, these experiments indicate that RNA decay in *Ascaris* extracts can lead to m^7Gp^*ppG and $m_3^{2,2,7}Gp^*ppG$ products. Both products are then substrates for a scavenger dinucleoside triphosphate hydrolase(s) that cleaves both cap structures.

Scavenger activity on mono- and trimethylated caps in *Ascaris* extracts

The scavenger decapping activity on $m^7Gp^*ppG_m$ and $m_3^{2,2,7}Gp^*ppG_m$ was further directly examined in the *Ascaris* embryo extracts using dinucleoside triphosphate substrates generated by P1 nuclease cleavage of cap-labeled

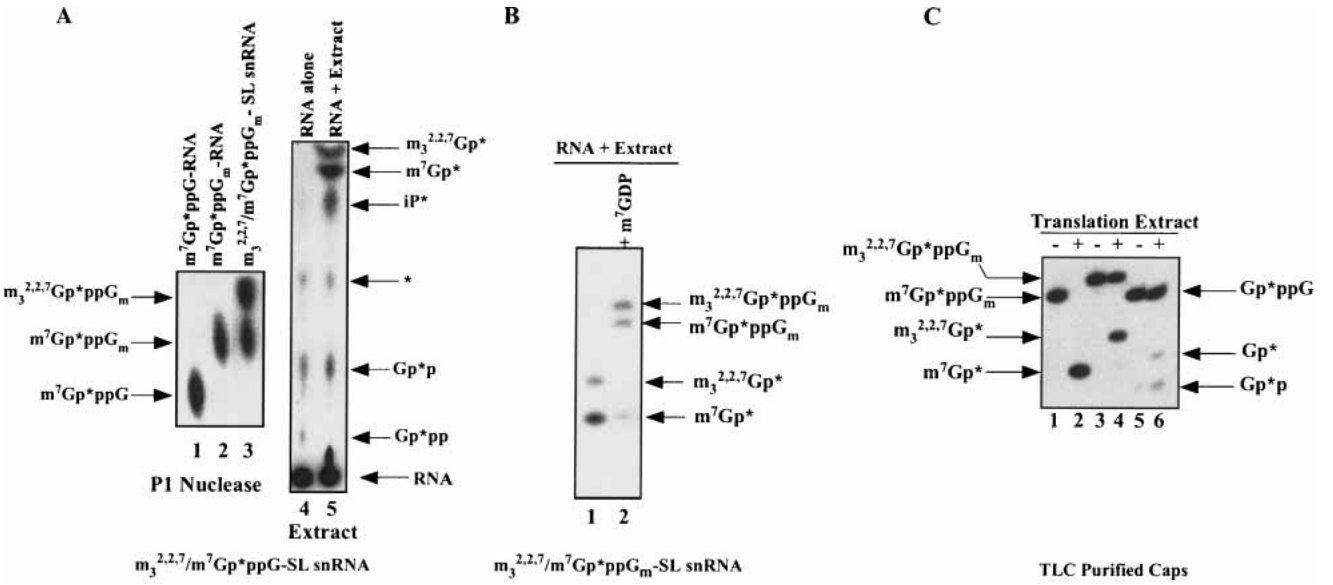

FIGURE 2. Decay and decapping of an $m_3^{2,2,7}$Gp*ppG/m^7Gp*ppG ^{32}P-cap-labeled RNA in *Ascaris* extracts leads to both m^7Gp* and $m_3^{2,2,7}$Gp* products. (*A*) Hypermethylation and decay of the SL snRNA in *Ascaris* extracts. Hypermethylation of the *Ascaris* SL snRNA in extracts leads to a mixed SL snRNA consisting of ~50% m^7Gp*ppG$_m$ SL snRNA and 50% $m_3^{2,2,7}$Gp*ppG$_m$ SL snRNA as illustrated by P1 nuclease digestion and TLC analysis of the released cap (see lane *3* and compare to lanes *1* and *2*; see also Supplementary Fig. 2A–C). Incubation of the mixed m^7Gp*ppG$_m$-/$m_3^{2,2,7}$Gp*ppG$_m$-SL snRNA in extracts leads to both m^7Gp* and $m_3^{2,2,7}$Gp* cap-derived products (see lane *5*) as illustrated by TLC and autoradiography. Although m^7GDP can comigrate with inorganic phosphate (iP) in this system, the product in lane *5* was shown to be iP based on the absence of its accumulation when phosphatase inhibitors were included in the reaction and the lack of conversion of this product to a triphosphate when incubated with nucleoside diphosphokinase (data not shown; Wang and Kiledjian 2001). Note that the Gp*p and Gp*pp spots are derived from the cap-labeling reaction and are not present in gel-purified RNA substrates that were used in other experiments with similar results. The reaction in lane *5* was carried with an approximately fivefold higher extract protein and longer incubation times than the reactions illustrated in Figure 1. * = unknown. (*B*) Inhibition of scavenger activity during decay reactions in *Ascaris* extracts leads to accumulation of methylated cap guanosine dinucleoside triphosphates. A mixed substrate, cap-labeled SL snRNA ($m_3^{2,2,7}$/m^7Gp*ppG$_m$-SL snRNA) was incubated in *Ascaris* extract with or without 100 μM m^7GDP, the reactions phenol:chloroform extracted, resolved by denaturing 25% PAGE, and detected by autoradiography. Decay and decapping of the substrate leads to accumulation of both m^7Gp* and $m_3^{2,2,7}$Gp* (see lane *1*). Inhibition of scavenger activity with 100 μM m^7GDP leads to accumulation of the substrates for the scavenger enzymes, m^7Gp*ppG$_m$ and $m_3^{2,2,7}$Gp*ppG$_m$ (lane *2*). Accumulation of a small amount of m^7Gp* results from incomplete inhibition of the scavenger activity in lane *2*. Note that PAGE assay is more sensitive than the TLC assay. (*C*) Scavenger activity in *Ascaris* translation extracts hydrolyzes $m_3^{2,2,7}$Gp*ppG$_m$. TLC purified cap-labeled substrates (see *A*; Supplementary Fig. 2A–D) were incubated with *Ascaris* extract, the reactions phenol:chloroform extracted, the reaction products resolved by 25% denaturing PAGE, and detected by autoradiography. The single, 30-min time-point assays were carried out within the linear range of extract concentration and incubation time using saturating substrate.

RNAs. The nematode scavenger activity was shown to cleave both m^7Gp*ppG$_m$ and $m_3^{2,2,7}$Gp*ppG$_m$ substrates (Fig. 2C, lanes 2,4). The scavenger hydrolase activity in *Ascaris* embryo extracts is robust, 5.3×10^{-12} mol/min/mg protein using 0.1 fmole of m^7Gp*ppG substrate. Extract scavenger activity is at least 50% less active on a $m_3^{2,2,7}$Gp*ppG$_m$ substrate compared to that observed with a m^7Gp*ppG$_m$ substrate (Fig. 2C, cf. lanes 2 and 4). Reduced activity of the scavenger enzyme on the trimethyl- compared to the monomethyl-cap substrate is supported by inhibition studies that indicate m^7GpppG is a stronger competitive inhibitor of the nematode scavenger activity than $m_3^{2,2,7}$GpppG (Table 1; data not shown). Scavenger hydrolysis of Gp*ppG in the extracts is low, demonstrating the activity has a preference for N^7-methylation of the cap (Fig. 2C, cf. lanes 2, 4, and 6). In addition, similar decay and decapping activities were also observed in *C. elegans* embryo extracts (Supplementary Fig. 2F; data not shown).

Direct RNA decapping and relative levels of scavenger and RNA decapping activities in *Ascaris* extracts

Direct RNA decapping of m^7Gp*ppG-RNA and $m_3^{2,2,7}$Gp*ppG$_m$-SL snRNA by a Dcp1/Dcp2 type activity producing m^7Gp*p and $m_3^{2,2,7}$Gp*p was also observed in *Ascaris* whole embryo extracts with the addition of Mn^{++} and the use of a more sensitive denaturing PAGE assay (Fig. 3, lanes 2,4). These assays were also carried out with either cold m^7GpppG or m^7GDP competitor to attempt to enhance and facilitate Dcp1/Dcp2 product formation as previously described (Gao et al. 2001). These cap analogs can inhibit scavenger decapping activity and sequester cap-binding proteins, which may facilitate better access of Dcp1/Dcp2 to the RNA cap. In general, use of cap analogs to sequester cap-binding proteins did not significantly enhance (≤twofold) our ability to detect potential Dcp1/Dcp2

TABLE 1. Competitive inhibitor analysis of recombinant nematode DcpS

Dinucleotide and nucleotide competitor	Approximate μM for 50% inhibition	
	C. elegans rDcpS	Human rDcpS
m^7GpppG	2.75	0.38
m^7GpppC	4	ND
m^7GpppU	4.5	ND
m^7GpppA	4	ND
m^7GpppG_m	8	ND
m^7GppppG	3	ND
m^7GTP	0.3	ND
m^7GDP	0.12	ND
m^7GMP	2.5	ND
$m_3^{2,2,7}$GpppG	64	8.5
$m_3^{2,2,7}$GpppA	76	ND
$m_3^{2,2,7}$GDP	>500	ND
GpppG	>500	ND
GDP	>500	ND
ApppG	>500	ND

Cap cleavage reactions were conducted at 30°C for 30 min with m^7Gp*ppG substrate and 10 ng of recombinant DcpS protein with different concentrations of dinucleoside triphosphate or nucleotide competitors (0.01–500 μM). Reaction products were resolved by TLC and detected by autoradiography. Assays were carried out within the linear range of protein, time, and using saturating substrate. Substrate to product conversion was analyzed with a Molecular Dynamics Storm 860 and ImageQuant software.
ND = Not determined.

activity and guanosine diphosphate product formation in the nematode extracts (Fig. 3, cf. lanes 2–5). Mn^{++} enhances the nematode extract Dcp1/Dcp2 activity (L.S. Cohen, M. Mikhli, C. Friedman, M. Jankowska-Anyszka, J. Stepinski, E. Darzynkiewicz, and R.E. Davis, unpubl.) as described for the yeast and human enzymes (Wang et al. 2002; Steiger et al. 2003). However, even in the presence of Mn^{++} (Fig. 3), we observed only relatively low levels of Dcp1/Dcp2 activity using a variety of extract preparations and different assay conditions. Although Dcp1/2 type activity and its products (m^7Gp*p and $m_3^{2,2,7}$Gp*p) are observed in the *Ascaris* extracts, the predominant decapping products observed are monophosphates consistent with a dinucleoside triphosphate or oligonucleotide "scavenger" decapping activity (DcpS). We estimate that the combined activity of 3′ to 5′ exoribonucleolytic decay of the RNA substrate and scavenger dinucleoside triphosphate hydrolysis of the resulting cap dinucleotides by the scavenger is at least ~15-fold greater (and ~60-fold in the absence of Mn^{++}) than the activity of Dcp1/Dcp2 RNA decapping activity in the extract (Fig. 3, lane 2; data not shown).

Overall, we have observed two types of decapping activities (scavenger- and Dcp1/Dcp2-like) in *Ascaris* extracts, each of which can cleave mono- and trimethylated caps. We have further shown that a recombinant *C. elegans* Dcp2 can directly decap $m_3^{2,2,7}$Gp*ppG_m-SL snRNA producing $m_3^{2,2,7}$Gp*p (Supplementary Fig. 1E, lanes 8,16).

Cap dinucleoside triphosphate hydrolase and RNA decapping activity in cellular fractions

To assess the distribution of the decapping enzyme activity in several cellular fractions, whole-cell embryo extracts were subjected to some initial fractionation as described in the Materials and Methods, and the fractions assayed for both DcpS and Dcp1/Dcp2 type activities. DcpS activity, assessed by dinucleoside cap cleavage leading to m^7Gp* or $m_3^{2,2,7}$Gp*, was observed in the 27,000 × *g* (S27) and 130,000 × *g* (S130) supernatant fractions, but reduced in the 130,000 × *g* pellet fractions and nuclear extracts (Fig. 4A,C). 3′ to 5′ exoribonuclease activity (producing cap dinucleoside triphosphate or combined with scavenger activity, m^7Gp* or $m_3^{2,2,7}$Gp*) was observed in all of the fractions examined, although lower levels were observed in nuclear extracts and the 130,000 × *g* pellet (Fig. 4B,C). Dcp1/Dcp2 RNA decapping activity was observed in all fractions including the S27 supernatant, S130 pellet, S130 pellet salt wash, and nuclear extracts (see Fig. 4B,C; data not shown) with the highest levels observed in the S130 pellet and S130 pellet salt wash. Thus, the two decapping activities exhibit differences in their cellular fractionation.

A *C. elegans* protein with scavenger DcpS activity

Because a DcpS ortholog likely carries out the scavenger activity observed in nematode extracts, we searched for and identified a putative *C. elegans* ortholog of the human DcpS in the *C. elegans*′ database. The *C. elegans* DcpS open reading frame was amplified by RT-PCR, cloned into a bacterial expression vector, and the bacterially expressed 6×-His-tagged protein purified by Ni^{2+}-NTA agarose and then ion exchange chromatography. The purified protein (>90% pure; Fig. 5A) is ribonuclease-free and readily cleaved m^7Gp*ppG dinucleoside triphosphate to m^7Gp* demonstrating that the identified *C. elegans* protein exhibited scavenger dinucleoside triphosphate hydrolase activity (Fig. 5B). The specific activity of the recombinant *C. elegans* DcpS for m^7Gp*ppG is $\sim 2 \times 10^{-11}$ moles/min/mg protein. A similarly purified recombinant human DcpS protein was also prepared and assayed for a comparison of activities and substrate specificity (see below; Fig. 5A).

C. elegans DcpS Hydrolyzes up to m^7Gp*ppG + 2 nucleotide substrates, but not longer substrates

To examine the substrate length requirement of the nematode DcpS, cap-labeled m^7Gp*ppGN_n oligonucleotide substrates of different lengths were prepared using nuclease P1 or RNase A digestion of different cap-labeled RNAs (see Materials and Methods). As illustrated in Figure 5C (lanes 7,8), m^7Gp*ppG and m^7Gp*ppG + 2 nucleotide substrates were readily cleaved to m^7Gp* by *C. elegans* DcpS, but dinucleoside triphosphate cap substrates with 3–6 addi-

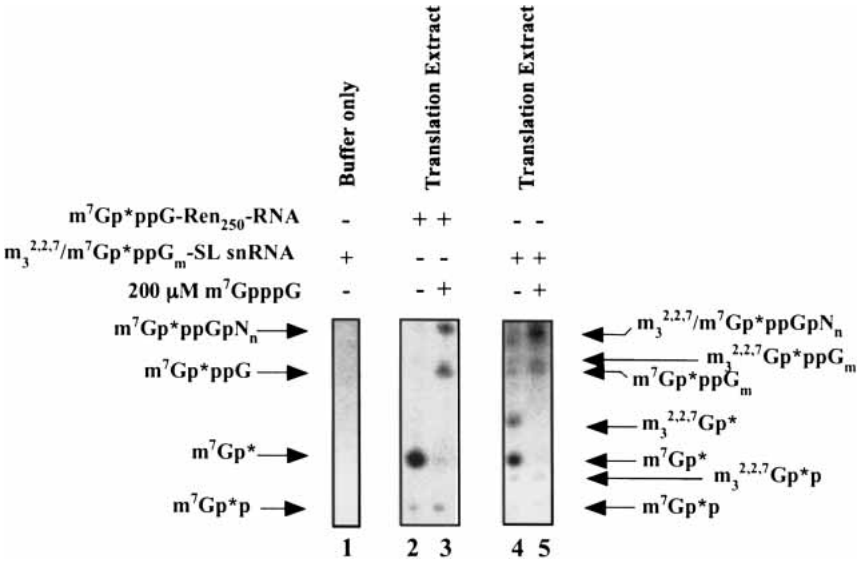

FIGURE 3. Dcp1/Dcp2 activity in *Ascaris* translation extracts. Cap-labeled RNAs were incubated in *Ascaris* translation extracts with and without 200 µM m^7GpppG, the reactions phenol:chloroform extracted, resolved by 25% denaturing PAGE, and products detected by autoradiography. Note the relative ratios of monophosphate (3′ to 5′ decay and scavenger activity) and diphosphate (Dcp1/Dcp2-like activity) nucleotide decay products in lanes 2 and 4. The diphosphate products do not increase dramatically when scavenger activity is inhibited with m^7GpppG. Dcp1/Dcp2 products (m^7Gp*p and $m_3^{2,2,7}$Gp*p), although limited, are highly reproducible.

tional 3′ nucleotides (lanes 9–12) were poor substrates for the dinucleoside triphosphate hydrolase activity. The recombinant human enzyme, by comparison, readily cleaves cap dinucleosides triphosphates with up to four additional nucleotides and retains some activity with m^7Gp*ppG + 6 oligonucleotide (Fig. 5C, lanes 13–18). These data on the human enzyme are in agreement with those described by Wang et al. (2002), who demonstrated that the human enzyme retains some activity on substrates as long as 10 nucleotides. Thus, nematode DcpS requires a shorter substrate than the human enzyme and exhibits minimal hydrolase activity on m^7Gp*ppG + 3 nucleotides or greater.

2′-O-Ribose is methylated in nematode caps

Capped RNAs from higher eukaryotes typically contain a 2′-O-methyl in the ribose of the first and second template encoded bases of the RNA (known as cap 2). Lower eukaryote mRNAs such as yeast do not have 2′-O-methyl added to the mRNA cap (Cap 0; Mager et al. 1976; Sripati et al. 1976). The *Ascaris* SL snRNA has an $m_3^{2,2,7}$GpppG$_m$ cap (cap 1) as shown by analysis of an in vivo ^{32}P-labeled SL snRNA (Maroney et al. 1990a,b). Transfer of the $m_3^{2,2,7}$GpppG$_m$ cap 1 with the 22 nucleotide spliced leader to mRNAs by *trans*-splicing (Liou and Blumenthal 1990; Van Doren and Hirsh 1990) would thus produce *trans*-spliced mRNAs with an $m_3^{2,2,7}$GpppG$_m$ (cap 1). As the $m_3^{2,2,7}$GpppG$_m$ cap is derived from a m^7GpppG-SL snRNA in vivo, it is likely that non-*trans*-spliced mRNAs in nematodes would have a m^7GpppN$_m$ cap (cap 1). In fact, we have observed 2′-O-ribose methylation of m^7GpppG-capped RNA in *Ascaris* extracts (data not shown).

C. elegans DcpS hydrolyzes both m^7GpppG and $m_3^{2,2,7}$GpppG (cap 0 and cap 1) dinucleoside triphosphate substrates

To further examine the substrate specificity of nematode DcpS, we prepared and TLC purified labeled m^7Gp*ppG, m^7Gp*ppG$_m$, $m_3^{2,2,7}$Gp*ppG, and $m_3^{2,2,7}$Gp*ppG$_m$ caps from cap-labeled RNAs treated with nuclease P1 (see Supplementary Fig. 2A–D). As we observed hydrolysis of both methylated and hypermethylated dinucleoside cap substrates in the *Ascaris* embryo extracts, we hypothesized that the *C. elegans* DcpS would cleave both m^7Gp*ppG and $m_3^{2,2,7}$Gp*ppG caps. As hypothesized, both substrates were in fact converted to their respective Gp* products (Fig. 6A, panels 1–3).

We then compared the substrate specificity of *C. elegans* and human DcpS for cap 0 and cap 1 m^7GpppG and $m_3^{2,2,7}$GpppG. As illustrated, both the nematode and human enzymes are active on either m^7GpppG cap 0 or cap 1 (Fig. 6A,B, panels 1,2). The *C. elegans* DcpS is also active on both cap 0 or cap 1 $m_3^{2,2,7}$GpppG (Fig. 6B, panel 3; data not shown). However, under similar assay conditions, the human DcpS enzyme did not hydrolyze either $m_3^{2,2,7}$GpppG cap 0 or cap 1 (Fig. 6, cf. A and B, panel 3; data not shown). Thus, the recombinant nematode DcpS has significant $m_3^{2,2,7}$GpppG hydrolase activity compared to the human enzyme. Furthermore, the 2′-O-methyl ribose does not significantly affect the activity of either the nematode or human DcpS.

C. elegans DcpS has minimal activity on a guanine dinucleoside triphosphate substrate that is not methylated (Gp*ppG) compared to methylated caps (Fig. 6A, panel 4). However, at ~100 ng recombinant protein a small, but detectable amount of Gp*ppG hydrolysis is observed. Very high levels of recombinant *C. elegans* DcpS protein (~500 ng) in an extended incubation lead to more efficient hydrolysis (see Supplementary Fig. 2D, lanes 5,8). Notably, the specificity for which phosphodiester bond is hydrolyzed appears reduced with the Gp*ppG substrate as both Gp* and Gp*p products are observed. Only monophosphate products are typically observed with methylated caps even with

excess DcpS protein. In comparison, up to 100 ng of human DcpS under the same assay conditions had almost no activity on a Gp*ppG substrate (Fig. 6B, cf. panel 4).

Competition experiments were also carried out using dinucleoside triphosphates and nucleotide competitors to gain further insight into the substrate specificity of the recombinant nematode DcpS enzyme. The concentration of competitor required to produce 50% inhibition of the recombinant enzyme is shown in Table 1. The most effective inhibitors were m^7GTP (0.3 μM) and m^7GDP (0.12 μM) nucleotides followed by m^7GMP (2.5 μM), then m^7GpppG/C/A/U (2.75, 4, 4, and 4.5 μM, respectively), m^7GppppG (3 μM), and m^7GpppG$_m$ (8 μM). Trimethylated guanine dinucleoside triphosphate substrates ($m_3^{2,2,7}$GpppG and $m_3^{2,2,7}$GpppA) were significantly less active as inhibitors (64 or 74 μM required for 50% inhibition). The 3′ nucleotide in a methylated guanine dinucleoside triphosphate does not lead to significant differences in level of inhibition. This is consistent with the likely variation in the +1 nucleotide of different non-*trans*-spliced mRNA transcripts. Neither ApppG nor nonmethylated guanine dinucleoside triphosphate (GpppG) or guanine nucleotides inhibited the enzyme. Interestingly, although trimethylated dinucleoside triphosphate substrates ($m_3^{2,2,7}$GpppG) can inhibit the enzyme, the trimethylated nucleotide diphosphate ($m_3^{2,2,7}$GDP) demonstrated minimal inhibition. In addition, nucleotide concentrations required for 50% inhibition of the nematode recombinant enzyme were in general approximately five- to eightfold higher than those observed for the human DcpS enzyme.

C. elegans DcpS binds to both m^7GTP- and $m_3^{2,2,7}$GTP-sepharose

The previous experiments indicated that *C. elegans* recombinant DcpS hydrolyzes $m_3^{2,2,7}$GpppG, whereas the human enzyme has minimal activity on this hypermethylated cap. To independently examine cap binding to mono- and trimethylguanosine nucleotides, cap-binding affinity experiments (Table 2) were carried out using the recombinant nematode and human DcpS enzymes and m^7GTP- and $m_3^{2,2,7}$GTP-Sepharose as previously described (Jankowska-Anyszka et al. 1998; Keiper et al. 2000; Miyoshi et al. 2002). The recombinant nematode DcpS protein bound with equivalent efficiency to the m^7GTP- and $m_3^{2,2,7}$GTP-Sepharose. In contrast, the human DcpS protein bound very poorly to $m_3^{2,2,7}$GTP-Sepharose and bound more tightly than *C. elegans* DcpS to the m^7GTP-Sepharose. As a positive control we used another nematode cap-binding protein, *Ascaris* eIF4E, which binds equally to both m^7GTP- and $m_3^{2,2,7}$GTP-Sepharose (S. Lall, C. Friedman, M. Jankowska-Anyszka, J. Stepinski, E. Darzynkiewicz, and R.E. Davis, in prep.). As negative controls that do not bind cap alone, we used *C. elegans* Dcp2 (L.S.

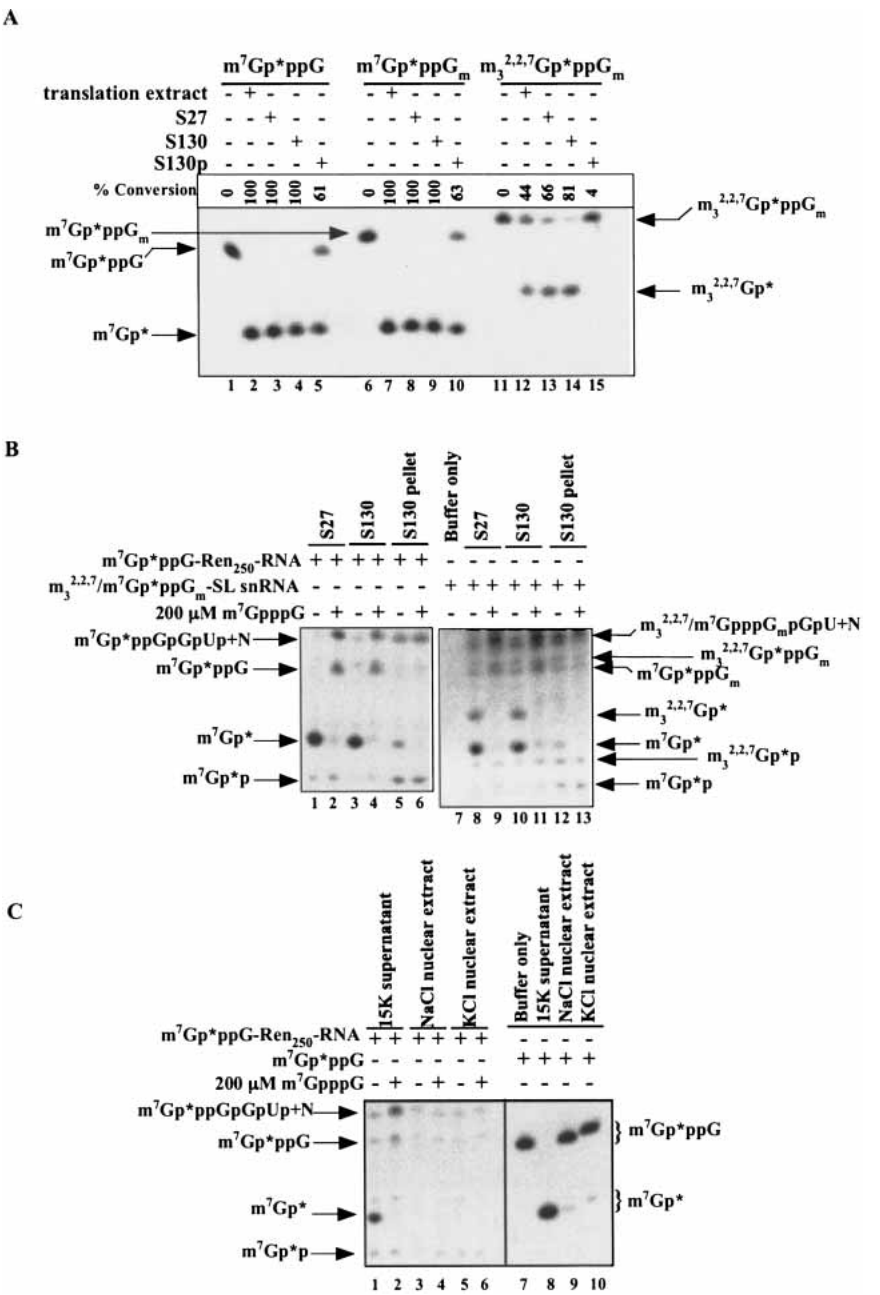

FIGURE 4. (Legend on next page)

Cohen, M. Mikhli, C. Friedman, M. Jankowska-Anyszka, J. Stepinski, E. Darzynkiewicz, and R.E. Davis, unpubl.) and nuclear cap-binding protein 80 (CBP80; R.E. Davis, unpubl.). These data are consistent with and provide additional experimental support to the cleavage studies (Fig. 6A,B, panel 3) that indicate the nematode DcpS has a higher affinity for trimethylated guanine nucleotides than does the human DcpS.

N^7-methyl guanosine diphosphate (m^7GDP) is a relatively poor substrate for *C. elegans* DcpS

Recently, experiments illustrating conversion of m^7GDP to m^7GMP by recombinant human DcpS were described (van Dijk et al. 2003). These studies suggested care should be taken in interpreting the contribution of different cellular decapping activities simply based on the accumulation of m^7GMP or m^7GDP products in cellular extracts because DcpS activity could be hydrolyzing the product of Dcp1/Dcp2 activity (e.g., m^7GDP) to m^7GMP. To determine whether the nematode extract and/or recombinant DcpS enzyme was active in the conversion of m^7GDP to m^7GMP, we generated and TLC purified m^7Gp*p substrate from m^7Gp*ppG-RNA using recombinant nematode Dcp2 (L.S. Cohen, M. Mikhli, C. Friedman, M. Jankowska-Anyszka, J. Stepinski, E. Darzynkiewicz, and R.E. Davis, unpubl.). Using similar assay conditions as described by van Dijk et al. (2003), we have not been able to observe significant conversion of m^7GDP to m^7GMP with either doubly purified, recombinant *C. elegans* or human DcpS preparations (Fig. 7A, panels 1 and 2). m^7Gp*ppG cap TLC purified during the same experiment is readily cleaved and mixing experiments indicate that the TLC purified m^7Gp*p added to an m^7Gp*ppG cleavage reaction does not contain TLC extracted components that inhibit the enzyme activity (Fig. 7B, panels 1,2; data not shown). Liu et al. (2002), in their characterization of the human protein, also noted that the human protein did not hydrolyze m^7GDP. Furthermore, in *Ascaris* whole-cell embryo extract assays, very little labeled m^7GDP is converted to m^7GMP (Fig. 7A, panels 3,4). The activity responsible for this conversion could be one of several different enzymes. Importantly, (1) the percentage of m^7GMP derived from m^7GDP in the extracts would contribute only a very small percentage of total m^7GMP to our in vitro decapping reactions, and (2) the levels of m^7GDP produced do not increase more than twofold in extract assays when DcpS is inhibited with m^7GpppG. This suggests it is unlikely the major m^7Gp* products observed in our whole embryo extract assays represent significant levels of DcpS conversion of m^7Gp*p derived from Dcp1/Dcp2 decapping of RNA, and that our estimates of the relative amounts of DcpS compared to Dcp1/Dcp2 activity are not subject to this limitation. Our interpretation of the data is that the predominant decay/decapping pathway in nematode embryos utilizes 3′ to 5′ exonuclease decay of the RNA followed by scavenger cleavage of the produced m^7GpppN and $m_3^{2,2,7}$GpppG dinucleoside triphosphates.

DISCUSSION

Summary

Analysis of decapping activities in nematode embryo extracts indicates the predominant activity is a scavenger decapping activity (DcpS-like) that hydrolyzes m^7GpppG and $m_3^{2,2,7}$GpppG products of 3′ to 5′ exoribonucleolytic RNA decay. Dcp1/Dcp2-like RNA decapping activity is detectable in nematode embryo extracts but present at significantly lower levels. Scavenger activity is very robust, and the combined activities of 3′ to 5′ exoribonucleolytic decay of RNA followed by N^7-guanosine nucleoside triphosphate hydrolase activities greatly exceeds (~15-fold) that observed for direct decapping of RNA by Dcp1/Dcp2-like activity. These data suggest that 3′ to 5′ decay appears to be the predominant general pathway of decay in nematode embryo extracts and may be the default pathway for mRNA degradation in vitro, at least for the RNA substrates examined.

Our characterization of *C. elegans* recombinant DcpS activity indicates the enzyme has limited activity on guanosine dinucleoside triphosphates (GpppG) unless the first base is methylated at the N^7 position. Nematode scavenger enzyme readily hydrolyzes m^7GpppG, m^7GpppG$_m$, m^7GpppGp, m^7GpppG$_m$p, and m^7GpppG$_m$pGp (some data not shown). Capped-oligonucleotides up to m^7GpppG + 2 nucleotides are actively hydrolyzed, but longer capped oligonucleotides are poor substrates. Nema-

FIGURE 4. Distribution of scavenger, 3′ to 5′ exoribonuclease, and Dcp1/Dcp2 activites in *Ascaris* embryo extract fractions. (*A*) Distribution of scavenger activity in fractionated *Ascaris* extracts. TLC purified cap substrates (derived from nuclease P1-treated RNA illustrated in Fig. 2A) were incubated in crudely fractionated *Ascaris* extract prepared as described in Materials and Methods and analyzed as described in Figure 3. S27 = 27,000 × *g* *Ascaris* embryo extract supernatant; S130 = 130,000 × *g* supernatant; S130 pellet = 130,000 × *g* pellet. (*B*) Dcp1/Dcp2-like and 3′ to 5′ decay/DcpS activity in fractionated *Ascaris* extracts. m^7Gp*ppG-Ren$_{250}$-RNA or mixed m^7Gp*ppG$_m$-/$m_3^{2,2,7}$Gp*ppG$_m$-SL snRNA was incubated in *Ascaris* embryo extract and analyzed as described in Figure 3. Exosome/DcpS activity is defined by the formation of m^7Gp* and $m_3^{2,2,7}$Gp*. Dcp1/Dcp2-like activity is defined as the formation of m^7Gp*p and $m_3^{2,2,7}$Gp*p. Note that both the DcpS and Dcp1/Dcp2 products are produced from the two capped RNA substrates. Hypermethylated SL snRNA is 50% monomethylated and 50% trimethylated as illustrated in Figure 2A, nuclease P1, lane *3*. The m^7Gp*p and $m_3^{2,2,7}$Gp*p products of Dcp1/Dcp2, although limited, are highly reproducible. It should be noted that Dcp2 has reduced activity on RNA substrates with the spliced leader sequence (L.S. Cohen, M. Mikhli, C. Friedman, M. Jankowska-Anyszka, J. Stepinski, E. Darzynkiewicz, and R.E. Davis, unpubl.), the substrate used to generate the hypermethylated cap. (*C*) 3′ to 5′ decay/DcpS, scavenger, and Dcp1/Dcp2 activity in nuclear extracts. m^7Gp*ppG-cap-labeled RNA (lanes *1–6*) or m^7Gp*ppG dinucleoside triphosphate (lanes *7–10*) was incubated in *Ascaris* embryo extract fractions and analyzed as described in Figure 3. Nuclear extracts were prepared as described in Materials and Methods.

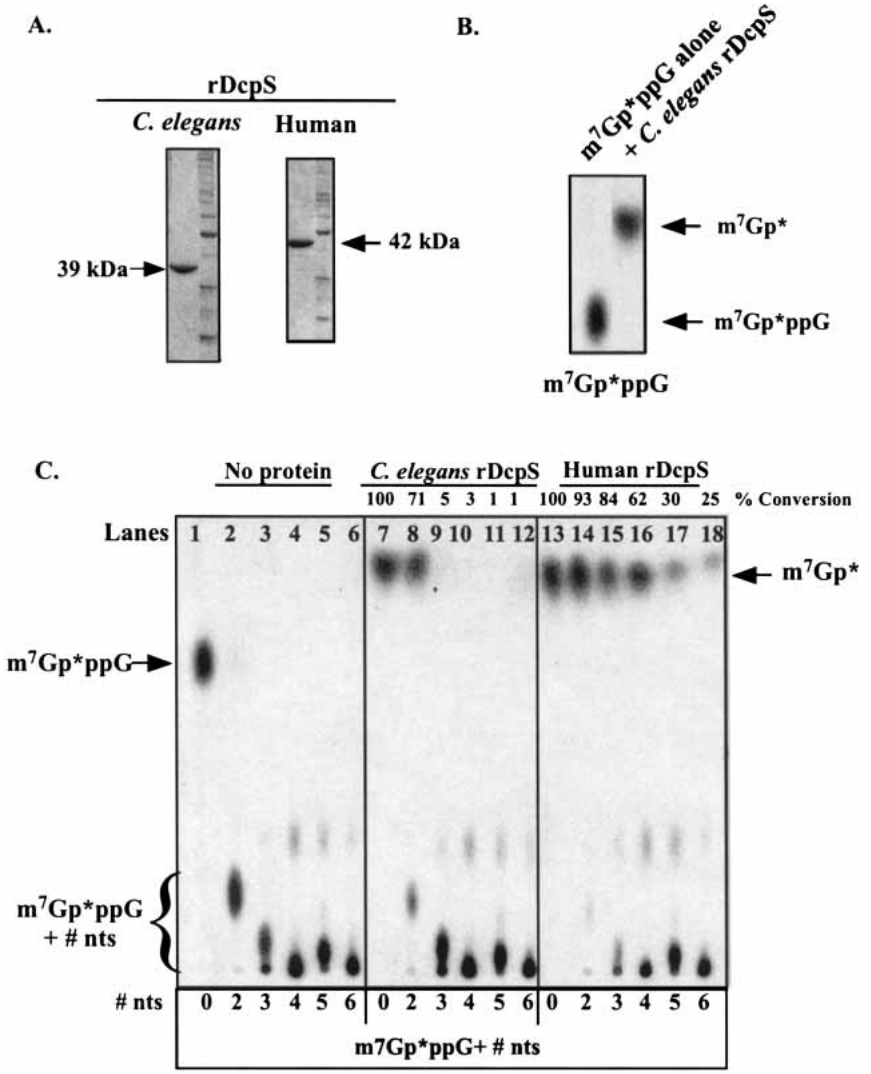

FIGURE 5. Recombinant nematode DcpS hydrolyzes free cap and maximum substrate length of recombinant nematode and human DcpS. (*A*) SDS-PAGE of recombinant DcpS proteins. Bacterially expressed, histidine tagged *C. elegans* and human DcpS were purified using nickel affinity and then Q-Sepharose Fast Flow column chromatography. Purified protein preparations were >90% pure based on Coomassie Blue staining of SDS-PAGE gels. (*B*) Recombinant *C. elegans* DcpS hydrolyzes m^7Gp^*ppG to m^7Gp^*. m^7Gp^*ppG in buffer alone or with 100 ng of recombinant DcpS protein was incubated for 30 min at 30°C and aliquots of the reactions applied to PEI-cellulose TLC plates, the plates developed in 0.45 M ammonium sulfate, and the substrate and product detected by autoradiography. (*C*) Maximum cap substrate length of recombinant nematode DcpS. Cap-labeled dinucleotide and oligonucleotide substrates were generated as described in the Materials and Methods. Cap cleavage reactions were carried out at 30°C for 30 min using 100 ng of recombinant protein and aliquots of the reactions applied to PEI-cellulose TLC plates, the plates developed in 0.45 M ammonium sulfate, and the substrate and product detected by autoradiography. Substrate to product conversion was determined from phosphoimager analysis. The substrate sequences are as follows: 0 = m^7GpppG_{OH}, +2 = $m^7GpppGpGpU_{OH}$, +3 = $m^7GpppGpGpGpC_{OH}$, +4 = $m^7GpppGpGpGpGpU_{OH}$, +5 = $m^7GpppGpGpGpApApC_{OH}$, and +6 = $m^7GpppGpGpApGpApC_{OH}$.

tode DcpS hydrolyzes tri-methyl-guanosine cap dinucleoside tri-phosphates including $m_3^{2,2,7}GpppG$, $m_3^{2,2,7}GpppG_m$, $m_3^{2,2,7}GpppGp$, and $m_3^{2,2,7}GpppG_mpGp$. Nematode DcpS is more active on m^7GpppG versus $m_3^{2,2,7}GpppG$, as illustrated by both direct hydrolysis of cap-labeled substrates (at least 2:1) and inhibition assays. Notably, in comparison, human DcpS has minimal activity on the trimethylated cap ($m_3^{2,2,7}GpppG$) and is active on longer oligonucleotide substrates. The data suggest there are differences between the human and nematode DcpS enzymes in the substrate binding pocket and/or its flexibility.

Structural basis for DcpS substrate requirements

Recently, the structure of human DcpS bound to m^7GpppG or m^7GpppA and insight into the mechanism of DcpS were reported (Gu et al. 2004). The DcpS structure indicates the protein is an asymmetric dimer that contains both an open nonproductive and a closed productive DcpS–cap complex. Many residues interact with the cap and/or each other to create a pocket that is favorable for m^7GpppG binding, as well as the structural changes associated with the closing of the pocket and subsequent cleavage of the cap. Differences in substrate and substrate length specificity observed among *Schizosaccharmyces pombe* (substrate can be a full-length capped RNA), nematodes (both m^7G- and $m_3^{2,2,7}GpppG$ cap and Cap + 2 nucleotides), and humans (Cap + 10 nucleotides) suggests that the binding pocket of DcpS enzymes exhibit unusual flexibility or distinct structural features associated with the open and closed conformations for cap binding and cleavage. It remains to be determined what overall structural determinants contribute to these differences.

We have identified a variety of additional DcpS orthologs in databases ranging from early eukaryotes (*Tetrahymena*, *Entamoeba*, *Chlamydomonas*, and a diatom) and metazoa including DcpS sequences from organisms with *trans*-splicing (tunicate: *Ciona*; flatworm: *Schistosoma*; *C. elegans*, and two additional parasitic nematodes: *Brugia malayi* and *Heterodera glycines*; data not shown). Comparison of these sequences (particularly DcpS orthologs from *trans*-splicing organisms) with the mechanistic and structural information derived from analysis of human DcpS will enable us to carry out

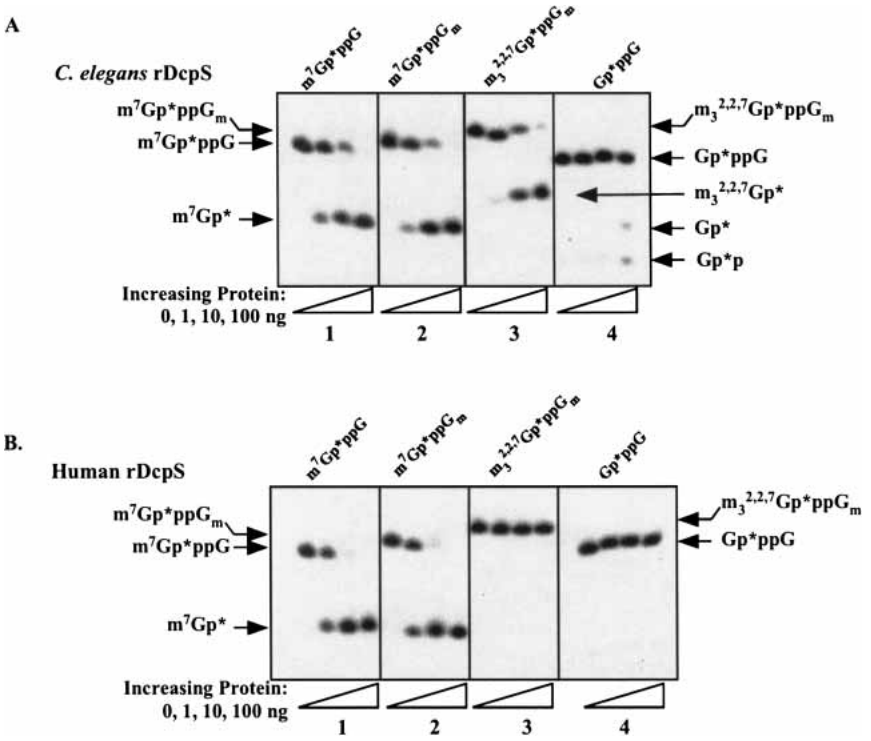

FIGURE 6. Comparison of cap substrate hydrolysis for recombinant *C. elegans* and human DcpS. Cap cleavage reactions were carried out at 30°C with recombinant *C. elegans* DcpS (*A*) or 37°C with recombinant human DcpS (*B*) for 30 min using TLC purified and characterized substrates. Reactions were carried out and analyzed as described in Figure 2C using 25% denaturing PAGE and detected by autoradiography. Control reactions using a similarly purified recombinant protein (β-galactosidase) demonstrated no degradation of RNA or cleavage of cap dinucleotides.

nematode DcpS structure/function studies that should provide insight into the difference in cap-binding specificity observed in nematodes, and if these differences may be exploitable for rational drug design in the development of new anti-nematode drugs.

Nematode scavenger activity and decapping of $m_3^{2,2,7}$GpppG-capped RNAs

During the course of our studies the characterization a *C. elegans* operon containing a histidine triad protein, dcs-1 was reported (Kwasnicka et al. 2003). This is the same protein we have characterized as *C. elegans* DcpS. Our data are in general agreement with their kinetic analysis and inhibition data indicating that the protein is relatively specific for N^7-methyl-guanine nucleotides. Their K_i values for m^7GpppG, m^7GTP, and m^7GDP were in the 2.2–3.5-μM range, and the K_i value for trimethylated cap was 28 μM, approximately eightfold higher than the monomethylated nucleotides. From their K_i data, Kwasnicka et al. (2003) concluded that the scavenger enzyme was not likely to function on $m_3^{2,2,7}$GpppG-capped snRNAs. Our data indicate that the protein can function on an $m_3^{2,2,7}$GpppG-capped snRNA, the SL snRNA, as well as a U1 snRNA (data not shown). In addition, of seminal importance in our view is whether the scavenger activity in nematodes is sufficient to act on $m_3^{2,2,7}$GpppG derived from *trans*-spliced mRNAs representing ~70% of the nematode mRNA population. Although the substrate affinity of nematode DcpS is clearly significantly lower for $m_3^{2,2,7}$GpppG than m^7GpppG, the levels of scavenger activity in nematode extracts are very high. DcpS activity associated with the exosome complex (or subset of exosome complex proteins) actively engaged in 3′ to 5′ RNA decay could also have altered kinetic properties, and might have access to higher local concentrations of substrate. Human DcpS activity was previously shown to be present both in free form and a complex, likely the exosome (Wang and Kiledjian 2001). We have made similar observations in the *Ascaris* extracts (data not shown). We have rarely observed significant accumulation of $m_3^{2,2,7}$GpppG or m^7GpppG caps in our embryo extract decay reactions (or in vivo following biolistic introduction of labeled RNAs; L.S. Cohen, M. Mikhli, C. Friedman, M. Jankowska-Anyszka, J. Stepinski, E. Darzynkiewicz, and R.E. Davis, unpubl.) where endogenous mRNAs in the extracts are simultaneously undergoing decay. Taken together, the high levels of nematode embryo DcpS-like activity, the in vitro decay data, and the likely association of DcpS with the exosome complex (data not shown) suggests to us that the activity in vivo is likely to be sufficient to hydrolyze both $m_3^{2,2,7}$GpppG and m^7GpppG caps derived from 3′ to 5′ decay. Alternatively, it remains possible that additional scavenger activities are present in nematodes that can hydrolyze trimethylguanosine

TABLE 2. Recombinant nematode DcpS binds to both m^7GTP- and $m_3^{2,2,7}$GTP-Sepharose

Recombinant protein	Cap analog affinity matrix	Relative binding affinity
C. elegans DcpS	m^7GTP-Sepharose	++
	$m_3^{2,2,7}$GTP-Sepharose	++
Human DcpS	m^7GTP-Sepharose	++++
	$m_3^{2,2,7}$GTP-Sepharose	–
Ascaris eIF4E	m^7GTP-Sepharose	+++
	$m_3^{2,2,7}$GTP-Sepharose	+++
C. elegans Dcp2	m^7GTP-Sepharose	–
or *C. elegans* CBP80	$m_3^{2,2,7}$GTP-Sepharose	–

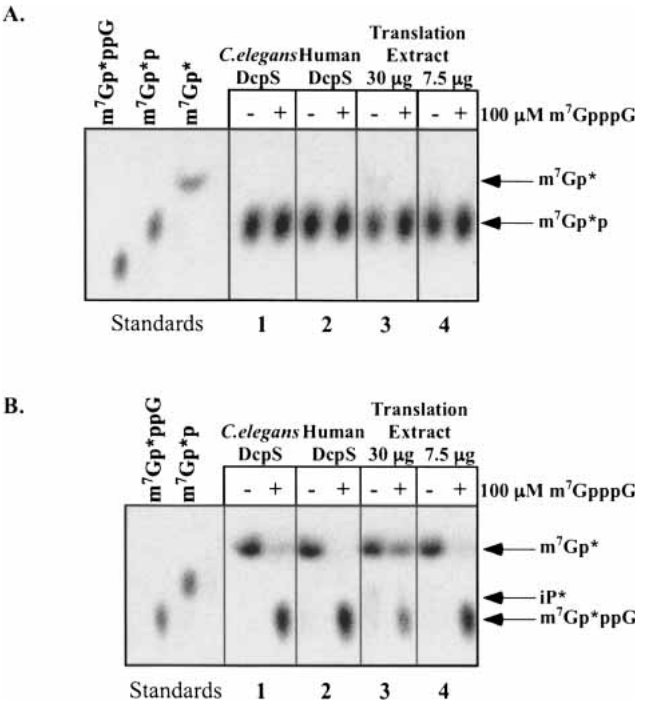

FIGURE 7. Recombinant nematode DcpS and *Ascaris* embryo extract activity on m^7GDP. Doubly purified recombinant *C. elegans* and human DcpS (150 ng) or *Ascaris* extract (30 and 7.5 µg) was incubated with TLC purified (*A*) m^7Gp*p or (*B*) m^7Gp*ppG and the reaction products analyzed by TLC and detected by autroradiography. Recombinant DcpS assays were carried out in a buffer as described (van Dijk et al. 2003) for 1 h with the human enzyme at 37°C and the nematode enzyme and extracts at 30°C. Reactions carried out with the decapping buffer used in the current study produced identical results. (*B*) Illustrates that a similarly purified substrate from the same experiment is a substrate for DcpS. Mixing experiment indicate that the TLC purified m^7Gp*p is not inhibitory to DcpS hydrolysis of m^7Gp*ppG in B (data not shown).

caps. Recently, a U8 snoRNA binding protein was identified as a nuclear decapping enzyme active on RNA substrates producing GDP (and its methylated derivatives) and p-RNA products (Ghosh et al. 2004). Although this protein can cleave $m_3^{2,2,7}$GpppG-capped RNA, and is conserved in vertebrates, it does not appear to be present in the genomes of lower eukaryotes including C. *elegans*.

Cellular distribution of decapping activities

Our initial extract studies suggest that the DcpS activity is primarily cytoplasmic in 32–64 cell *Ascaris* embryos. Studies by the Kiledjian laboratory (Liu et al. 2002) also found that the human DcpS protein was primarily found in the cytoplasmic fraction, with little protein observed in the nuclear fraction based on immunoprecipitation experiments. However, analysis of the *S. pombe*, COS cell, and human DcpS proteins using fluorescence and immunocytochemistry indicate that they localize primarily to the nucleus (Salehi et al. 2002; Kwasnicka et al. 2003; Cougot et al. 2004; M. Kiledjian, pers. comm.). The predominantly nuclear localization of the COS cell DcpS led Kwasnicka et al. (2003) to propose that the enzyme might function to decap aberrant transcripts in the nucleus that might result under stress conditions. Studies are currently underway in our laboratory to examine the localization of DcpS protein using immunocytochemistry in developing nematode embryos and to examine the interaction of nematode DcpS with other cap-binding proteins and exosome components.

Conclusion

The nematode-decapping enzymes, DcpS and Dcp1/Dcp2, have the ability to hydrolyze the typical eukaryotic m^7GpppG cap as well as the $m_3^{2,2,7}$GpppG cap added to mRNAs through *trans*-splicing. An in vitro decay system is described that indicates RNA decay by a 3′ to 5′ pathway followed by DcpS hydrolysis of the resulting cap appears to be the predominant nematode decay pathway in embryo extracts. These studies provide the foundation for further studies to characterize the contribution and interplay of translation and decay in the expression of *trans*-spliced and non-*trans*-spliced nematode mRNAs.

MATERIALS AND METHODS

Preparation of whole-cell embryo and nuclear extracts

Whole-cell extracts were prepared from 32–64 cell *Ascaris suum* embryos using methods similar to those described by Nilsen and collaborators (Hannon et al. 1990a,b; Maroney et al. 1995) with a metal dounce, 10 mM KCl, and protease inhibitors. These *Ascaris* embryo extracts are competent for cap-dependent translation and exhibit mRNA cap and poly(A)-tail synergism (S. Lall, C. Friedman, M. Jankowska-Anyszka, J. Stepinski, E. Darzynkiewicz, and R.E. Davis, in prep.). In some experiments, extracts were prepared with a modified buffer system (10 mM Tris-HCl, pH 7.5, 1 mM KoAc, 1.5 mM MgoAc, 1 mM DTT, and protease inhibitors) and crudely fractionated as described (Brewer and Ross 1990; Ross 1999; Wang and Kiledjian 2000). *Ascaris* embryo nuclear extracts were prepared as described (Seidl and Moritz 1998), the nuclear pellets extracted with either 400 mM KCl or 350 mM NaCl, and the resulting nuclear extracts dialyzed. *C. elegans* whole-cell embryo extracts were generously provided by Margaret MacMorris and Tom Blumenthal.

Transcription template and RNA preparation

PCR templates (see Supplementary Fig. 1) for in vitro transcription reactions were prepared from Promega plasmid pRLnull or pAscSL_snRNA using primers provided in the Supplementary Figure 1. These PCR reactions generate templates with a T7 promoter, different 5′ UTRs with or without the spliced leader sequence, and 3′ ends either with or without a poly(A) tail or a homopolymeric 3′ G_{16} tract. Transcription reactions produced from either a Riboprobe or MegaScript kit as described by the manufacturer (Promega and Ambion) were DNase I-treated, extracted with TRIzol Reagent (Invitrogen), and the RNAs precipitated twice, once with isopropanol and then with ammonium acetate/ethanol. Precipitated RNAs were further washed with 70% ethanol, dissolved in

water, quantitated spectrophotometrically, and examined by agarose-formaldehyde, denaturing gel electrophoresis.

Cap-labeled substrate preparation

Cap-labeled RNAs were prepared from uncapped RNA substrates using ^{32}P-α-GTP (Perkin-Elmer), and recombinant vaccinia RNA guanylyltransferase and (guanine- N^7)-methyltransferase (generously provided by Stewart Shuman) or human capping enzyme (generously provided by Aaron Shatkin). In some experiments, the cap was further methylated at the 2′-O-ribose by inclusion of mRNA cap-specific 2′-O-methyltransferase (generously provided by Paul Gershon). For many experiments, cap-labeled RNAs were gel purified by denaturing PAGE prior to use.

Cap-labeled oligonucleotides of defined length (see Fig. 5C) were derived by treating cap-labeled RNA transcripts (derived from pRLnull, pBlueScript II SK, pGL3 Basic, or the Megascript positive control template) with RNase A and characterized prior to use by thin layer chromatography (TLC) and PAGE.

Cap dinucleoside triphosphates (Gp*ppG, m^7Gp*ppG or $m_3^{2,2,7}$Gp*ppG, where the * follows the ^{32}P-labeled phosphate) were typically generated from cap-labeled RNAs by Nuclease P1 (Calbiochem and Sigma) digestion of the RNA (see Supplementary Fig. 2A,B). In some cases, caps were produced from cap-labeled RNAs by T1 digestion (Ambion), which produces caps or capped oligonucleotides with a 3′ phosphate. To generate pure cap-labeled substrates, labeled RNAs and caps were either gel purified or purified by TLC and elution of individual substrates in 1× decapping buffer.

Ascaris $m_3^{2,2,7}$Gp*ppG_m-SL snRNA was produced by hypermethylation of an m^7Gp*ppG_m-SL snRNA in *Ascaris* whole-cell embryo extracts and purified as previously described (Maroney et al. 1990b).

Whole cell extract decay analysis

Ascaris embryo extract mRNA decay and decapping assays were carried out using the decapping buffer of Zhang et al. (1999) (50 mM Tris, pH 7.9, 30 mM $(NH_4)_2SO_4$, 1 mM $MgCl_2$, 1 mM DTT) with the addition of 2.5 mM $MnCl_2$, which increases Dcp2 activity. RNA substrates in the reactions ranged from ~0.04–13 ng (0.5–163 fmole) per reaction, corresponding to 5000–160,000 dpm. Cap dinucleoside triphosphate substrates (e.g., m^7Gp*ppG, m^7Gp*ppG_m, or their nonmethylated or hypermethylated derivatives) ranged from ~500–64,000 dpm/reaction (0.05–0.64 fmole). Reactions typically contained 7.5 μg of protein (protein range in reactions was ~2–30 μg), the reactions were incubated at 30°C for 30–60 min, and then extracted with 1:1 phenol:chloroform/isoamyl alcohol. For specific activity determinations, reactions were carried out within the linear range of protein and time using a set substrate concentration described in the text. Reactions were spotted onto TLC plates or loaded on denaturing PAGE gels, resolved as described below, and detected by autoradiography.

Cloning, expression, and purification of *C. elegans* DcpS

Total *C. elegans* RNA was isolated from mixed stage *C. elegans* cultures using Trizol®. First-strand cDNA was generated using SuperScript II reverse transcriptase and oligo dT primers (Invitrogen). The *C. elegans* DcpS open reading frame was amplified from the cDNA using specific primers (see Supplementary Fig. 1) and Expand High Fidelity Polymerase (Roche). The DcpS coding region PCR product was digested with NdeI and BamHI (Promega) and cloned into pET16b (Novagen) using DH5α as a host. Recombinants were identified and confirmed by DNA sequencing. Clones were then transformed into Rosetta DE3 (Novagen) for protein expression. Protein expression was induced with 0.4 mM isopropyl β-D-thiogalactoside overnight at room temperature. Frozen bacterial pellets were resuspended in ice-cold lysis buffer (20 mM HEPES, pH 7.5, 300 mM NaCl, 300 mM urea, 10% glycerol, 1% Triton X-100, 10 mM imidazole), lysozyme was added to a final concentration of 1 mg/mL, the suspension incubated on ice for 30 min, and then sonicated. The 6×-His-tagged DcpS was bound to Ni^{2+}-nitrilotriacetic acid (NTA)-agarose (Qiagen Inc.) for 60 min at 4°C, unbound proteins removed with a washing buffer (20 mM HEPES, pH 7.5, 300 mM NaCl), and the bound proteins eluted with wash buffer containing increasing concentrations of imidazole (20–300 mM imidazole). Fractions containing DcpS were dialyzed against 20 mM Tris pH 7.5, 150 mM NaCl, loaded onto a HiTrap Q FF anion exchange column (Pharmacia) equilibrated in the same buffer, and bound protein eluted with a gradient from 0.15 to 1 M NaCl. Those fractions containing DcpS activity were dialyzed against 0.2 mM EDTA, 20 mM Tris, pH 7.5, 50 mM KCl, 20% glycerol, 1 mM DTT, 0.5 mM PMSF and stored at –80°C. Human DcpS in pET28, generously provided by Kiledjian et al. (Liu et al. 2002), was expressed and purified in a manner identical to the nematode protein.

Recombinant DcpS assay

Recombinant DcpS cap cleavage assays were carried out as described for the embryo extracts at 30°C for 30 min with ~1–150 ng of two step purified (His-Tag and anion exchange) recombinant protein. Inhibition assays contained unlabeled dinucleoside triphosphates and guanosine nucleoside phosphates that were premixed in reaction buffer before the addition of the protein. DcpS reactions were stopped on ice, extracted with phenol/chloroform, the reaction products resolved on TLC plates or PAGE gels, and detected by autoradiography. Substrate to product conversion was determined by phosphoimager analysis using Molecular Dynamics STORM 860 and ImageQuant software. For the inhibition experiments, 50% inhibition was determined by graphical analysis of percent conversion of substrate to product and determination of the amount of inhibitor needed for 50% inhibition.

Substrate characterization and dinucleoside triphosphate (cap) cleavage and RNA decapping product analysis

Capped RNA and cap substrates and their reaction products were characterized and identified using a variety of methods including comigration with known standards using TLC or denaturing PAGE analysis and several enzyme shift strategies (treatment with alkaline phosphatase [Roche], phosphatase inhibitors [Sigma], diphosphonucleotide kinase [Sigma], tobacco acid pyrophosphatase [Epicentre], nucleotide pyrophosphatase [Sigma], Nuclease P1 [Calbiochem], Nuclease T1 [Ambion], and RNase A [Ambion]) (see Supplementary Fig. 2; data not shown). TLC was carried out using PEI-cellulose as the stationary phase and ammonium sulfate (0.45 M) or lithium chloride (0.75 M) as the mobile phase. PAGE

analysis was done using 20% or 25% denaturing gels as described (Bergman et al. 2002). Reaction substrates and products were then quantified by phosphoimager analysis of the TLC or PAGE separations using Molecular Dynamics STORM 860 and ImageQuant software.

m^7GTP- and $m_3^{2,2,7}$GTP-sepharose binding assays

Recombinant *C. elegans* DcpS, human DcpS, *C. elegans* Dcp2 (L.S. Cohen, M. Mikhli, C. Friedman, M. Jankowska-Anyszka, J. Stepinski, E. Darzynkiewicz, and R.E. Davis, unpubl.), *Ascaris* eIF4E (S. Lall, C. Friedman, M. Jankowska-Anyszka, J. Stepinski, E. Darzynkiewicz, and R.E. Davis, unpubl.), and *C. elegans* CBP80 (R.E. Davis, unpubl.) were mixed with m^7GTP-Sepharose or $m_3^{2,2,7}$GTP-Sepharose beads (Jankowska et al. 1993) in binding buffer (20 mM Tris, pH 7.5, 25 mM KCl, 0.2 mM EDTA, 1 mM DTT, 0.5 mM PMSF, 20% glycerol), the samples incubated for 45 min at 4°C with gentle shaking, the sepharose beads washed with binding buffer, and the bound proteins eluted with binding buffer containing 500 mM KCl. Proteins that remained bound to the sepharose beads were removed from the beads by denaturation using heat and Laemmli SDS PAGE loading buffer. Aliquots of the proteins (starting material, flow-through, wash, and eluate) were analyzed by SDS PAGE, stained with SYPRO Ruby (Molecular Probes), and analyzed with a Molecular Dynamics Storm 860 and ImageQuant software.

Other reagents

The following dinucleoside cap analogs were synthesized as previously described: m^7GpppG, GpppG, m^7GppppG, and $m_3^{2,2,7}$GpppG, according to Stepinski et al. (1995), and m^7GpppC, m^7GpppU, m^7GpppA, and m^7GpppG$_m$, according to Jankowska et al. (1996). ApppG and $m_3^{2,2,7}$GpppA were prepared by a new recently developed strategy (Stepinski et al. 2001) using adenosine 5′-phoshorimidazolide and GDP and $m_3^{2,2,7}$GDP, respectively, as substrates and carrying out the coupling reaction in dimethylformamide in the presence of zinc chloride. Nucleotide competitors m^7GMP, m^7GDP, m^7GTP, and $m_3^{2,2,7}$GDP were prepared from GMP, GDP, GTP, and $m_2^{2,2}$GDP, respectively, by the methylation method described earlier (Darzynkiewicz et al. 1985). The synthesis of m^7GTP- and $m_3^{2,2,7}$GTP-Sepharose 4B were also carried out by the known method (Jankowska et al. 1993).

ELECTRONIC SUPPLEMENTARY DATA

Supplementary material can be found online at http://www.uchsc.edu/sm/bbgn/Davislab/RNA_DcpS.html.

ACKNOWLEDGMENTS

Human DcpS coding region in pET-28a (pET28-hDcpS) was generously provided by Mike Kiledjian, recombinant vaccinia RNA guanylyltransferase and (guanine-N^7)-methyltransferase by Stewart Shuman, human RNA guanylyltransferase by Aaron Shatkin, mRNA cap-specific 2′-O-methyltransferase by Paul Gershon, and *C. elegans* whole embryo extract by Margaret MacMorris and Tom Blumenthal. We thank Mike Kiledjian and his laboratory for exceptionally helpful discussions and sharing reagents and information. Thanks to Carol J. Wilusz and Jeffrey Wilusz for generously providing reagents, information, and encouragement. Thanks to Paul Copeland and Scott Kinzy for helping us to carry out gel filtration experiments in their laboratory, and to Chris Lima and Mike Kiledjian for access to data prior to publication. We thank members of the Davis lab for their comments on the manuscript. This work was supported by National Institutes of Health (NIH) Grant AI49558 and CUNY-CSI startup funds to R.E.D., and Grants #PBZ-KBN-059/T09/10 and KBN 3 P04A 021 25 from the Polish Committee for Scientific Research to E.D.

The publication costs of this article were defrayed in part by payment of page charges. This article must therefore be hereby marked "advertisement" in accordance with 18 USC section 1734 solely to indicate this fact.

Received May 6, 2004; accepted June 24, 2004.

REFERENCES

Anderson, J.S.J. and Parker, R.P. 1998. The 3′ to 5′ degradation of yeast mRNAs is a general mechanism for mRNA turnover that requires the SKI2 DEVH box protein and 3′ to 5′ exonucleases of the exosome complex. *EMBO J.* **17:** 1497–1506.

Beelman, C.A., Stevens, A., Caponigro, G., LaGrandeur, T.E., Hatfield, L., Fortner, D.M., and Parker, R. 1996. An essential component of the decapping enzyme required for normal rates of mRNA turnover. *Nature* **382:** 642–646.

Bergman, N., Opyrchal, M., Bates, E.J., and Wilusz, J. 2002. Analysis of the products of mRNA decapping and 3′-to-5′ decay by denaturing gel electrophoresis. *RNA* **8:** 959–965.

Blumenthal, T. and Gleason, K.S. 2003. *Caenorhabditis elegans* operons: Form and function. *Nat. Rev. Genet.* **4:** 110–118.

Brewer, G. and Ross, J. 1990. Messenger RNA turnover in cell-free extracts. *Methods Enzymol.* **181:** 202–209.

Chen, C.Y., Gherzi, R., Ong, S.E., Chan, E.L., Raijmakers, R., Pruijn, G.J., Stoecklin, G., Moroni, C., Mann, M., and Karin, M. 2001. AU binding proteins recruit the exosome to degrade ARE-containing mRNAs. *Cell* **107:** 451–464.

Cougot, N., Babajko, S., and Seraphin, B. 2004. Cytoplasmic foci are sites of mRNA decay in human cells. *J. Cell Biol.* **165:** 31–40.

Darzynkiewicz, E., Ekiel, I., Tahara, S.M., Seliger, L.S., and Shatkin, A.J. 1985. Chemical synthesis and characterization of 7-methylguanosine cap analogs. *Biochemistry* **24:** 1701–1707.

Decker, C.J. and Parker, R. 2002. mRNA decay enzymes: Decappers conserved between yeast and mammals. *Proc. Natl. Acad. Sci.* **99:** 12512–12514.

Denker, J.A., Maroney, P.A., Yu, Y.T., Kanost, R.A., and Nilsen, T.W. 1996. Multiple requirements for nematode spliced leader RNP function in *trans*-splicing. *RNA* **2:** 746–755.

Denker, J.A., Zuckerman, D.M., Maroney, P.A., and Nilsen, T.W. 2002. New components of the spliced leader RNP required for nematode *trans*-splicing. *Nature* **417:** 667–670.

Dunckley, T. and Parker, R. 1999. The DCP2 protein is required for mRNA decapping in *Saccharomyces cerevisiae* and contains a functional MutT motif. *EMBO J.* **18:** 5411–5422.

Ferguson, K.C., Heid, P.J., and Rothman, J.H. 1996. The SL1 *trans*-spliced leader RNA performs an essential embryonic function in *Caenorhabditis elegans* that can also be supplied by SL2 RNA. *Genes & Dev.* **10:** 1543–1556.

Gao, M., Wilusz, C.J., Peltz, S.W., and Wilusz, J. 2001. A novel mRNA-decapping activity in HeLa cytoplasmic extracts is regulated by AU-rich elements. *EMBO J.* **20:** 1134–1143.

Ghosh, T., Peterson, B., Tomasevic, N., and Peculis, B.A. 2004. *Xenopus* U8 snoRNA binding protein is a conserved nuclear decapping enzyme. *Mol. Cell* **13:** 817–828.

Gingras, A.C., Raught, B., and Sonenberg, N. 1999. eIF4 initiation factors: effectors of mRNA recruitment to ribosomes and regulators of translation. *Annu. Rev. Biochem.* **68:** 913–963.

Gu, M., Fabrega, C., Liu, S.-W., Liu, H., Kiledjian, M., and Lima, C.D. 2004. Insights into the structure, mechanism and regulation of scavenger decapping activity. *Mol. Cell* **14:** 67–80.

Hannon, G.J., Maroney, P.A., Ayers, D.G., Shambaugh, J.D., and Nilsen, T.W. 1990a. Transcription of a nematode *trans*-spliced leader RNA requires internal elements for both initiation and 3′ end-formation. *EMBO J.* **9:** 1915–1921.

Hannon, G.J., Maroney, P.A., Denker, J.A., and Nilsen, T.W. 1990b. Trans splicing of nematode pre-messenger RNA in vitro. *Cell* **61:** 1247–1255.

He, F., Li, X., Spatrick, P., Casillo, R., Dong, S., and Jacobson, A. 2003. Genome-wide analysis of mRNAs regulated by the nonsense-mediated and 5′ to 3′ mRNA decay pathways in yeast. *Mol. Cell* **12:** 1439–1452.

Huang, X.Y. and Hirsh, D. 1989. A second *trans*-spliced RNA leader sequence in the nematode *Caenorhabditis elegans*. *Proc. Natl. Acad. Sci.* **86:** 8640–8644.

Izaurralde, E., Lewis, J., McGuigan, C., Jankowska, M., Darzynkiewicz, E., and Mattaj, I.W. 1994. A nuclear cap binding protein complex involved in pre-mRNA splicing. *Cell* **78:** 657–668.

Izaurralde, E., Lewis, J., Gamberi, C., Jarmolowski, A., McGuigan, C., and Mattaj, I.W. 1995. A cap-binding protein complex mediating U snRNA export. *Nature* **376:** 709–712.

Jankowska, M., Temeriusz, A., Stolarski, R., and Darzynkiewicz, E. 1993. Synthesis of m2,7GTP- and m2,2,7GTP-Sepharose 4B: New affinity resins for isolation of cap binding proteins. *Collect. Czech. Chem. Commun.* **58:** 132–137.

Jankowska, M., Stepinski, J., Stolarski, R., Wieczorek, Z., Temeriusz, A., Haber, D., and Darzynkiewicz, E. 1996. ^{1}H NMR and fluorescence studies of new mRNA 5′-cap analogues. *Collect. Czech. Chem. Commun.* **61:** S197–SS202.

Jankowska-Anyszka, M., Lamphear, B.J., Aamodt, E.J., Harrington, T., Darzynkiewicz, E., Stolarski, R., and Rhoads, R.E. 1998. Multiple isoforms of eukaryotic protein synthesis initiation factor 4E in *Caenorhabditis elegans* can distinguish between mono- and trimethylated mRNA cap structures. *J. Biol. Chem.* **273:** 10538–10542.

Keiper, B.D., Lamphear, B.J., Deshpande, A.M., Jankowska-Anyszka, M., Aamodt, E.J., Blumenthal, T., and Rhoads, R.E. 2000. Functional characterization of five eIF4E isoforms in *Caenorhabditis elegans*. *J. Biol. Chem.* **275:** 10590–10596.

Kwasnicka, D.A., Krakowiak, A., Thacker, C., Brenner, C., and Vincent, S.R. 2003. Coordinate expression of NADPH-dependent flavin reductase, Fre-1, and Hint-related 7meGMP-directed hydrolase, DCS-1. *J. Biol. Chem.* **278:** 39051–39058.

LaGrandeur, T.E. and Parker, R. 1998. Isolation and characterization of Dcp1p, the yeast mRNA decapping enzyme. *EMBO J.* **17:** 1487–1496.

Lejeune, F., Li, X., and Maquat, L.E. 2003. Nonsense-mediated mRNA decay in mammalian cells involves decapping, deadenylating, and exonucleolytic activities. *Mol. Cell* **12:** 675–687.

Liou, R.F. and Blumenthal, T. 1990. *Trans*-spliced *Caenorhabditis elegans* mRNAs retain trimethylguanosine caps. *Mol. Cell. Biol.* **10:** 1764–1768.

Liu, Y., Huang, T., MacMorris, M., and Blumenthal, T. 2001. Interplay between AAUAAA and the *trans*-splice site in processing of a *Caenorhabditis elegans* operon pre-mRNA. *RNA* **7:** 176–181.

Liu, H., Rodgers, N.D., Jiao, X., and Kiledjian, M. 2002. The scavenger mRNA decapping enzyme DcpS is a member of the HIT family of pyrophosphatases. *EMBO J.* **21:** 4699–4708.

Lykke-Andersen, J. 2002. Identification of a human decapping complex associated with hUpf proteins in nonsense-mediated decay. *Mol. Cell. Biol.* **22:** 8114–8121.

Mager, W.H., Klootwijk, J., and Klein, I. 1976. Minimal methylation of yeast messenger RNA. *Mol. Biol. Rep.* **3:** 9–17.

Maroney, P.A., Hannon, G.J., Denker, J.A., and Nilsen, T.W. 1990a. The nematode spliced leader RNA participates in *trans*-splicing as an Sm snRNP. *EMBO J.* **9:** 3667–3673.

Maroney, P.A., Hannon, G.J., and Nilsen, T.W. 1990b. Transcription and cap trimethylation of a nematode spliced leader RNA in a cell-free system. *Proc. Natl. Acad. Sci.* **87:** 709–713.

Maroney, P.A., Denker, J.A., Darzynkiewicz, E., Laneve, R., and Nilsen, T.W. 1995. Most mRNAs in the nematode *Ascaris lumbricoides* are *trans*-spliced: A role for spliced leader addition in translational efficiency. *RNA* **1:** 714–723.

Milone, J., Wilusz, J., and Bellofatto, V. 2002. Identification of mRNA decapping activities and an ARE-regulated 3′ to 5′ exonuclease activity in trypanosome extracts. *Nucleic Acids Res.* **30:** 4040–4050.

———. 2004. Characterization of deadenylation in trypanosome extracts and its inhibition by poly(A)-binding protein Pab1p. *RNA* **10:** 448–457.

Miyoshi, H., Dwyer, D.S., Keiper, B.D., Jankowska-Anyszka, M., Darzynkiewicz, E., and Rhoads, R.E. 2002. Discrimination between mono- and trimethylated cap structures by two isoforms of *Caenorhabditis elegans* eIF4E. *EMBO J.* **21:** 4680–4690.

Mukherjee, D., Gao, M., O'Connor, J.P., Raijmakers, R., Pruijn, G., Lutz, C.S., and Wilusz, J. 2002. The mammalian exosome mediates the efficient degradation of mRNAs that contain AU-rich elements. *EMBO J.* **21:** 165–174.

Newbury, S. and Woollard, A. 2004. The 5′-3′ exoribonuclease xrn-1 is essential for ventral epithelial enclosure during *C. elegans* embryogenesis. *RNA* **10:** 59–65.

Nilsen, T.W. 2001. Evolutionary origin of SL-addition *trans*-splicing: Still an enigma. *Trends Genet.* **17:** 678–680.

Nuss, D.L. and Furuichi, Y. 1977. Characterization of the m7G(5′)pppN-pyrophosphatase activity from HeLa cells. *J. Biol. Chem.* **252:** 2815–2821.

Nuss, D.L., Furuichi, Y., Koch, G., and Shatkin, A.J. 1975. Detection in HeLa cell extracts of a 7-methyl guanosine specific enzyme activity that cleaves m7GpppNm. *Cell* **6:** 21–27.

Parker, R. and Song, H. 2004. The enzymes and control of eukaryotic mRNA turnover. *Nat. Struct. Mol. Biol.* **11:** 121–127.

Piccirillo, C., Khanna, R. and Kiledjian, M. 2003. Functional characterization of the mammalian mRNA decapping enzyme hDcp2. *RNA* **9:** 1138–1147.

Ross, J. 1999. Assays for analyzing exonucleases in vitro. *Methods* **17:** 52–59.

Salehi, Z., Geffers, L., Vilela, C., Birkenhager, R., Ptushkina, M., Berthelot, K., Ferro, M., Gaskell, S., Hagan, I., Stapley, B., et al. 2002. A nuclear protein in *Schizosaccharomyces pombe* with homology to the human tumour suppressor Fhit has decapping activity. *Mol. Microbiol.* **46:** 49–62.

Seidl, C. and Moritz, K.B. 1998. A novel UV-damaged DNA binding protein emerges during the chromatin-eliminating cleavage period in *Ascaris suum*. *Nucleic Acids Res.* **26:** 768–777.

Spieth, J., Brooke, G., Kuersten, S., Lea, K., and Blumenthal, T. 1993. Operons in *C. elegans*: Polycistronic mRNA precursors are processed by *trans*-splicing of SL2 to downstream coding regions. *Cell* **73:** 521–532.

Sripati, C.E., Groner, Y., and Warner, J.R. 1976. Methylated, blocked 5′ termini of yeast mRNA. *J. Biol. Chem.* **251:** 2898–2904.

Steiger, M., Carr-Schmid, A., Schwartz, D.C., Kiledjian, M., and Parker, R. 2003. Analysis of recombinant yeast decapping enzyme. *RNA* **9:** 231–238.

Stepinski, J., Bretner, M., Jankowska, M., Felczak, K., Stolarski, R., Wieczorek, Z., Cai, A.-L., Rhoads, R.E., Temeriusz, A., Haber, D., et al. 1995. Synthesis and properties of P^1,P^2-, P^1,P^3- and P^1,P^4-dinucleoside di-, tri- and tetraphosphate mRNA 5′-cap analogues. *Nucleosides Nucleotides* **14:** 717–721.

Stepinski, J., Waddell, C., Stolarski, R., Darzynkiewicz, E., and Rhoads, R.E. 2001. Synthesis and properties of mRNAs containing the novel "anti-reverse" cap analogs 7-methyl(3′-O-methyl)GpppG and 7-methyl (3′-deoxy)GpppG. *RNA* **7:** 1486–1495.

Tucker, M. and Parker, R. 2000. Mechanisms and control of mRNA decapping in *Saccharomyces cerevisiae*. *Annu. Rev. Biochem.* **69:** 571–595.

van Dijk, E., Cougot, N., Meyer, S., Babajko, S., Wahle, E., and Seraphin, B. 2002. Human Dcp2: A catalytically active mRNA de-

capping enzyme located in specific cytoplasmic structures. *EMBO J.* **21:** 6915–6924.

van Dijk, E., Le Hir, H., and Seraphin, B. 2003. DcpS can act in the 5′-3′ mRNA decay pathway in addition to the 3′-5′ pathway. *Proc. Natl. Acad. Sci.* **100:** 12081–12086.

Van Doren, K. and Hirsh, D. 1990. mRNAs that mature through *trans*-splicing in *Caenorhabditis elegans* have a trimethylguanosine cap at their 5′ termini. *Mol. Cell. Biol.* **10:** 1769–1772.

Von Der Haar, T., Gross, J.D., Wagner, G., and McCarthy, J.E. 2004. The mRNA cap-binding protein eIF4E in post-transcriptional gene expression. *Nat. Struct. Mol. Biol.* **11:** 503–511.

Wang, Z. and Kiledjian, M. 2000. Identification of an erythroid-enriched endoribonuclease activity involved in specific mRNA cleavage. *EMBO J.* **19:** 295–305.

———. 2001. Functional link between the mammalian exosome and mRNA decapping. *Cell* **107:** 751–762.

Wang, Z., Jiao, X., Carr-Schmid, A., and Kiledjian, M. 2002. The hDcp2 protein is a mammalian mRNA decapping enzyme. *Proc. Natl. Acad. Sci.* **99:** 12663–12668.

Williams, C., Xu, L., and Blumenthal, T. 1999. SL1 trans splicing and 3′-end formation in a novel class of *Caenorhabditis elegans* operon. *Mol. Cell. Biol.* **19:** 376–383.

Zhang, S., Williams, C.J., Wormington, M., Stevens, A., and Peltz, S.W. 1999. Monitoring mRNA decapping activity. *Methods* **17:** 46–51.

Zorio, D.A., Cheng, N.N., Blumenthal, T., and Spieth, J. 1994. Operons as a common form of chromosomal organization in *C. elegans*. *Nature* **372:** 270–272.